

Electronic Supplementary Information

Mixed crystal formation of two gold isocyanide complexes with various ratios for continuous tuning of photophysical properties

Tomohiro Seki,^{a*} Naoki Toyoshima,^a Hajime Ito^{a,b*}

^aDivision of Applied Chemistry & Frontier Chemistry Center (FCC), Faculty of Engineering, Hokkaido University, Sapporo, Hokkaido 060-8628, Japan

^bInstitute for Chemical Reaction Design and Discovery (WPI-ICReDD), Hokkaido University, Sapporo, Hokkaido 060-8628, Japan.

seki@eng.hokudai.ac.jp

hajito@eng.hokudai.ac.jp

Contents	
1. General	S2
2. Synthesis	S3
3. Photophysical Properties of Solid Sample of 1, 2, and 1·2	S5
4. XRD Analyses and Bending Properties of 1	S6
5. Emission Spectra, XRD Analyses and Bending Properties of 2	S7
6. Single Crystal X-ray Structure Analyses	S9
7. ¹⁹F NMR spectra of 1, 2 and 1·2	S14
8. Emission and Bending Properties of 1·2	S16
9. NMR Spectra	S19
10. References	S22

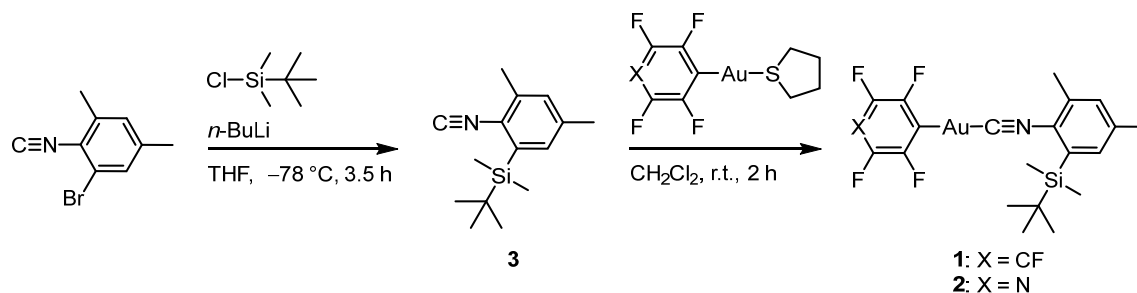
1. General

All commercially available reagents and solvents are of reagent grade and were used without further purification unless otherwise noted. Solvents for the synthesis were purchased from commercial suppliers, degassed by three freeze-pump-thaw cycles and further dried over molecular sieves (4 Å). NMR spectra were recorded on a JEOL JNM-ECX400P or JNM-ECS400 spectrometer (^1H : 400 MHz; ^{13}C : 98.5 MHz; ^{19}F : 373 MHz) using tetramethylsilane and CDCl_3 as internal standards, respectively. Emission spectra were measured by using an Olympus fluorescence microscope BX51 equipped with Hamamatsu photonics multichannel analyzer PM-12. The powder samples were loaded into an aluminum pan and sealed and were cooled inside the apparatus. Elemental analyses and low- and high-resolution mass spectra were recorded at the Global Facility Center at Hokkaido University. Photographs were obtained using OLYMPUS BX51 or SZX7 microscopes with Olympus DP72, Nikon D5100 or RICOH CX1 digital cameras. Powder diffraction data were recorded at on a Rigaku SmartLab diffractometer with $\text{Cu-K}\alpha$ radiation and D/teX Ultra detector covering $5\text{--}60^\circ$ (2θ).

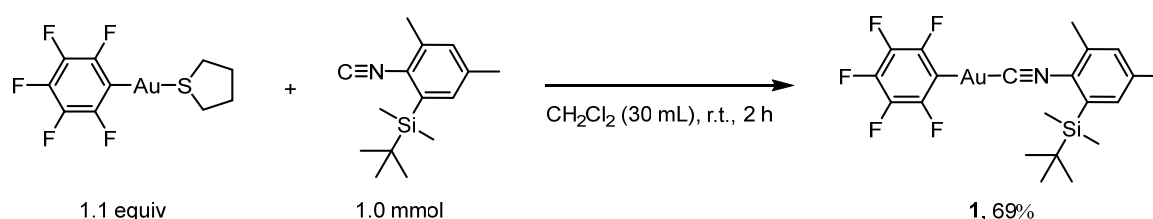
X-ray diffraction analyses: Single crystal X-ray structural analyses were carried out on a Rigaku XtaLAB PRO MM007 or XtaLAB-Synergy diffractometer using graphite monochromated $\text{Mo-K}\alpha$ or $\text{Cu-K}\alpha$ radiation. The structure was solved by direct methods and expanded using Fourier techniques. Non-hydrogen atoms were refined anisotropically. Hydrogen atoms were refined using the riding model. All calculations were performed using the Olex2 crystallographic software package except for refinement, which was performed using SHELXL-2018.¹ Simulated powder patterns were generated with Mercury 4.1² from the structures determined by the single-crystal diffraction analyses.

2. Synthesis

Scheme S1 Synthesis of **1** and **2**.

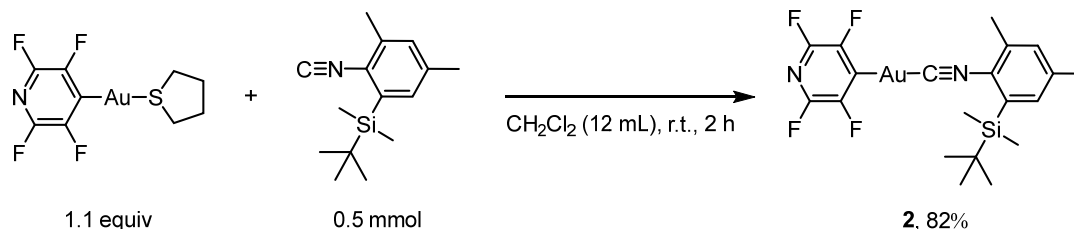


Synthesis of **1**



A mixture of pentafluorophenyl(tetrahydrothiophen)gold(I)³ (497.1 mg, 1.1 mmol) and silyl isocyanide **3** (248.5 mg, 1.0 mmol) was stirred in CH₂Cl₂ (30 mL) for 2 h under nitrogen at room temperature. After the reaction completion was monitored by TLC analysis, the solvent was removed with a rotary evaporator under a reduced pressure. The residues are washed with methanol, which gave analytically pure **1** as white solid (416.6 mg, 0.70 mmol, 69 %). ¹H NMR (400 MHz, CDCl₃, Fig. S16, δ): 0.45 (s, 6H), 0.95 (s, 9H), 2.39 (s, 3H), 2.45 (s, 3H), 7.18 (s, 2H). ¹³C NMR (98.5 MHz, CDCl₃, Fig. S17, δ): -4.5 (CH₃), 18.3 (C), 19.2 (C), 21.6 (CH₃), 26.6 (CH₃), 126.5–126.82(m, C), 132.5 (CH), 135.0 (CH), 135.5–135.8 (m, C), 136.0 (C), 136.6 (C), 138.0–138.5 (m, C), 140.7 (C), 148.1–148.5 (m, C), 150.4–150.8 (m, C), 159.8–160.4 (m, C). ¹⁹F NMR (373 MHz, CDCl₃, Fig. S11, δ): -162.88 to -163.01 (m, 2F), -157.97 to -158.07 (m, 1F), -116.33 to -116.44 (m, 2F). MS-ESI (*m/z*): [M+Na]⁺ calcd for C₂₁H₂₃AuF₅NSiNa, 632.10831; found, 632.10826. Elemental analysis (calcd, found for C₂₁H₂₃AuF₅NSi): C (41.39, 41.17), H (3.80, 3.81), N (2.30, 2.26).

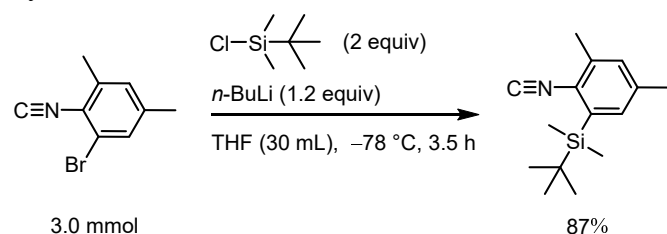
Synthesis of **2**



A mixture of 2,4,5,6-tetrafluoropyridine(tetrahydrothiophen)gold(I)⁴ (240.2 mg, 0.55mmol) and 2,4-dimethyl-6-*tert*-butyldimethylsilylisocyanobenzene (121.9 mg, 0.5 mmol) was stirred in CH₂Cl₂ (12

mL) for 2 h under nitrogen at room temperature. After the reaction completion was monitored by TLC analysis, the solvent was removed with a rotary evaporator under a reduced pressure. The residues are washed with methanol, which gave analytically pure **2** as white solid (240.9 mg, 0.41 mmol, 82 %). ¹H NMR (400 MHz, CDCl₃, Fig. S18, δ): 0.45 (s, 6H), 0.96 (s, 9H), 2.39 (s, 3H), 2.46 (s, 3H), 7.19 (s, 2H). ¹³C NMR (98.5 MHz, CDCl₃, Fig. S19, δ): -4.5 (CH₃), 18.4 (C), 19.2 (C), 21.6 (CH₃), 26.6 (CH₃), 126.4 (br, C), 132.5 (CH), 135.1 (CH), 136.1 (C), 136.6 (C), 141.0 (C), 143.2 (d with complicated couplings, *J* = 246.4 Hz, C), 146.0 (d with complicated couplings, *J* = 239.9 Hz, C), 152.1 (t, *J* = 50.0 Hz, C), 158.9–159.4 (m, C). ¹⁹F NMR (373 MHz, CDCl₃, Fig. S11, δ): -121.81 to -122.01 (m, 2F), -96.57 to -96.76 (m, 2F). MS-ESI (*m/z*): [M+H]⁺ calcd for C₂₀H₂₄AuF₄N₂Si, 593.13104; found, 593.13077. Elemental analysis (calcd, found for C₂₀H₂₃AuF₄N₂Si): C (40.55, 40.45), H (3.91, 3.91), N (4.73, 4.66).

Synthesis of **3**



A powder of 2-bromo-4,6-dimethylisocyanobenzene⁵ (631.1mg, 3.0 mmol) was placed in an oven-dried two-neck flask. The flask was connected to a vacuum/nitrogen manifold through a rubber tube. It was evacuated and then backfilled with nitrogen. This cycle was repeated three times. THF (30 mL) was then added in the flask through the rubber septum using a syringe. After cooling to -78 °C, *n*-BuLi in hexane (2.3 ml, 3.6 mmol, 1.57 M) was added dropwise and then added *tert*-butyldimethylchlorosilane (901.0 mg 6.0 mmol). After stirred for 3.5 h at -78 °C, and allowed to warm to room temperature. Then, reaction mixture was extracted with CH₂Cl₂ three times and washed with H₂O. The organic layers were collected and dried over MgSO₄. After filtration, the solvent was removed with a rotary evaporator under a reduced pressure. The residue was purified by column chromatography (ethyl acetate/dichloromethane) over silica gel to give compound **3** as white solid (637.8 mg, 87 %). ¹H NMR (400 MHz, CDCl₃, Fig. S20, δ): 0.42 (s, 6H), 0.94 (s, 9H), 2.33 (s, 3H), 2.38 (s, 3H), 7.09 (s, 2H). ¹³C NMR (98.5 MHz, CDCl₃, Fig. S21, δ): -4.6 (CH₃), 18.3 (C), 19.5 (CH₃), 21.3 (CH₃), 26.8 (CH₃), 129.3 (br, C), 131.9 (CH), 134.1 (C), 134.3 (CH), 135.2 (C), 137.9 (C), 167.0 (C). MS-ESI (*m/z*): [M+H]⁺ calcd for C₁₅H₂₄N₁Si, 246.16725; found, 246.16709.

3. Photophysical Properties of Solid Samples of 1, 2, and 1·2

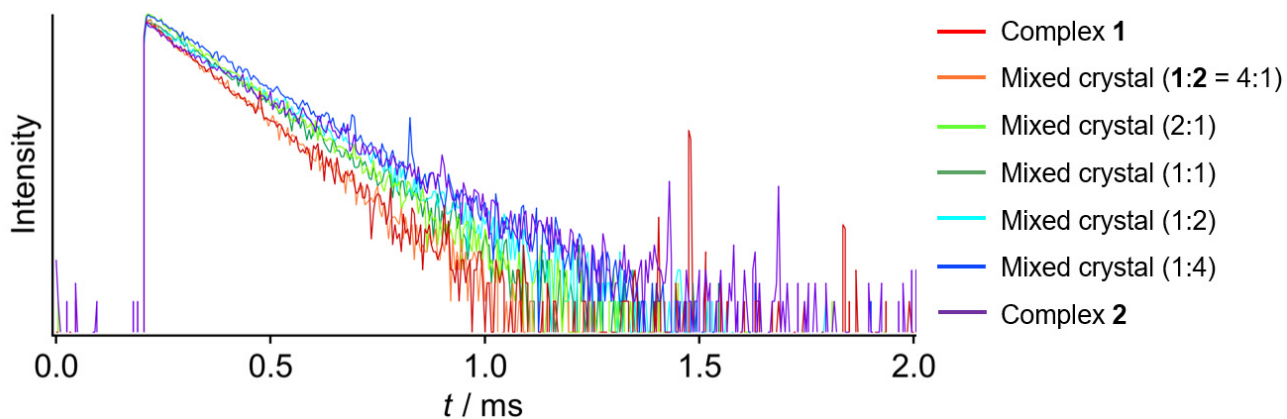


Fig. S1 Emission decay profiles of 1, 2, and 1·2.

Table S1 Absolute emission quantum yield Φ_{em} and mean emission lifetime of 1, 2, and 1·2.

	$\Phi_{em} / -$ (λ_{ex} / nm)	$\tau_{av} / \mu\text{s}^{a,b,c}$	$\tau_1 / \mu\text{s}$ ($A / -$)	$\tau_2 / \mu\text{s}$ ($A / -$)
1	0.57 (310)	130	130 (0.51)	0.00043 (0.49)
1·2 (4:1)	0.69 (302)	130	130 (0.87)	32 (0.13)
1·2 (2:1)	0.66 (302)	150	150 (0.51)	0.95 (0.49)
1·2 (1:1)	0.68 (300)	150	160 (0.77)	120 (0.23)
1·2 (1:2)	0.69 (305)	170	170 (0.47)	0.00070 (0.53)
1·2 (1:4)	0.78 (309)	180	190 (0.53)	96 (0.47)
2	0.79 (300)	190	200 (0.78)	57 (0.22)

^a $\lambda_{ex} = 370 \text{ nm}$. ^b $\lambda_{em} = 432 \text{ nm}$. ^c $\tau_{av} = \Sigma(A_n\tau_n^2) / \Sigma(A_n\tau_n)$.

4. XRD Analyses and Bending Properties of **1**

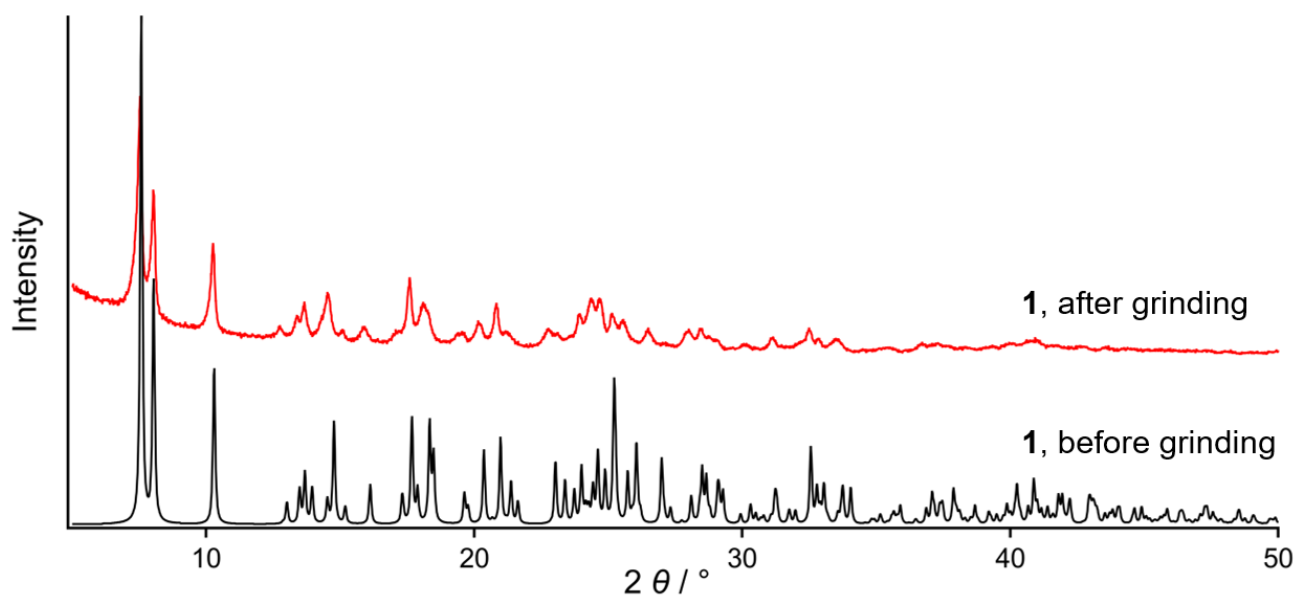


Fig. S2 Simulated powder XRD pattern of **1** (black line) derived from the single crystal structure and experimentally obtained powder XRD pattern of the ground powder of **1** (red line).

Note: The peak positions of the PXRD pattern of the ground phase are almost the same as the simulated pattern of the unground phase without the appearance of the new peaks. Together with the small intensity of the peaks of the powder pattern of ground phase, the mechanical grinding induces the crystal-to-amorphous phase transitions.

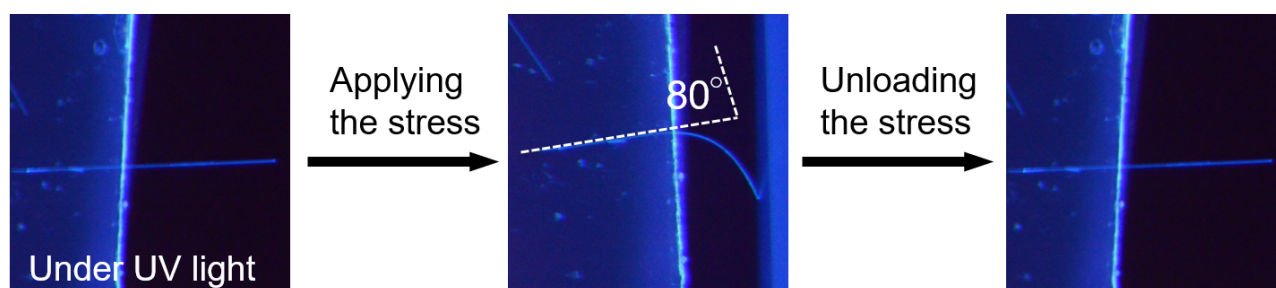


Fig. S3 Photographs of the crystals of **1** showing elastic bending property under gentle mechanical stimulation recorded under UV light.

5. Emission Spectra, XRD Analyses and Bending Properties of 2

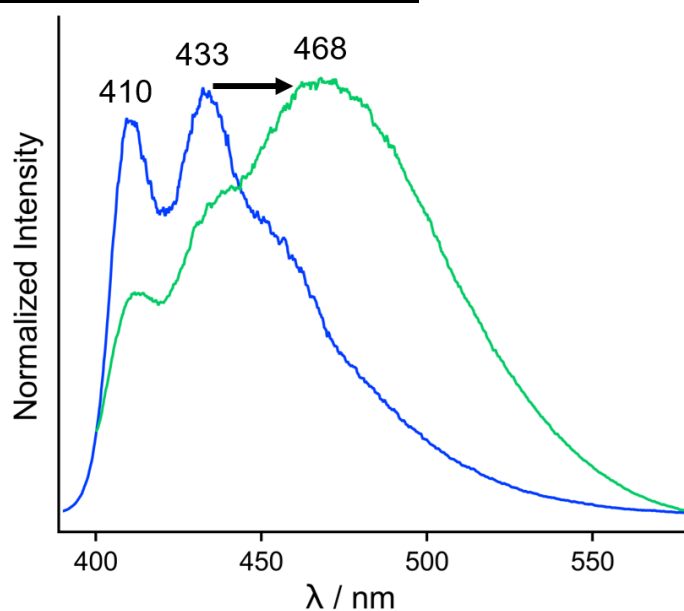


Fig. S4 Emission spectra of the solid sample of **2** before (blue line) and after (green line) mechanical stimulation ($\lambda_{\text{ex}} = 365 \text{ nm}$).

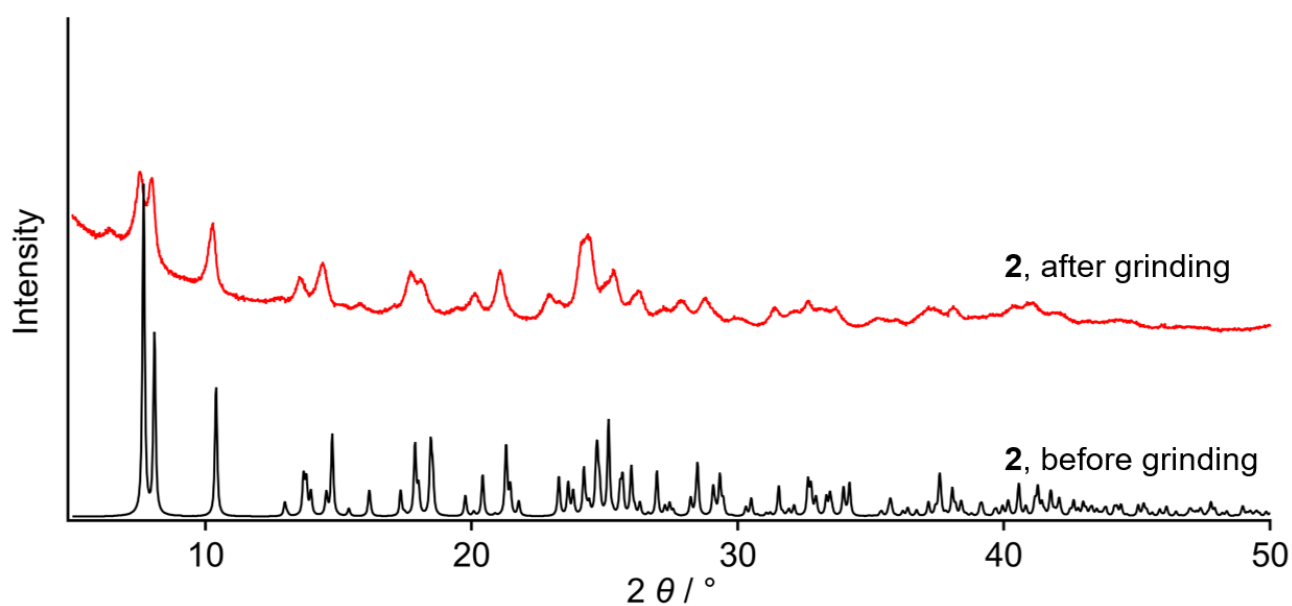


Fig. S5 Simulated powder XRD pattern of **2** (black line) derived from the single crystal structure and experimentally obtained powder XRD pattern of the ground powder of **2** (red line).

Note: The peak positions of the PXRD pattern of the ground phase are almost the same as the simulated pattern of the unground phase without the appearance of the new peaks. Together with the small intensity of the peaks of the powder pattern of ground phase, the mechanical grinding induces the crystal-to-amorphous phase transitions.

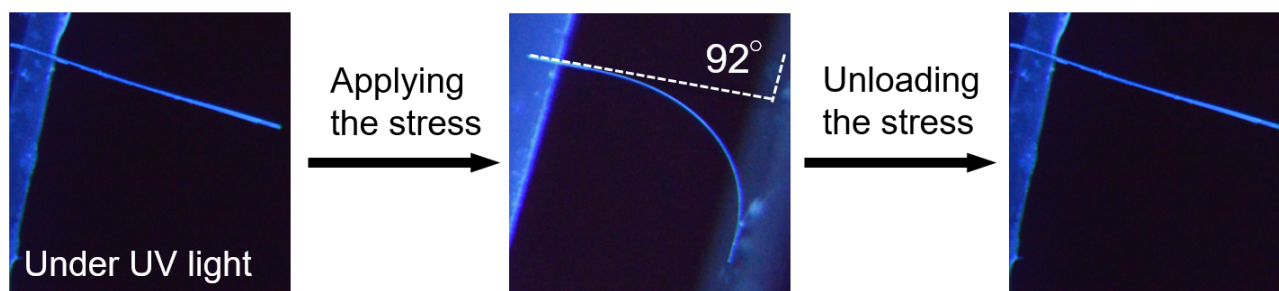


Fig. S6 Photographs of the crystals of **2** showing elastic bending property under gentle mechanical stimulation recorded under UV light.

6. Single Crystal X-ray Structure Analyses

Table S2. Summary of X-ray crystallographic data for **1**, **2** and **1·2**

compound	1	2	1·2
CCDC Number	CCDC 1953581	CCDC 1953582	CCDC 1953583
Empirical Formula	C ₂₁ H ₂₃ AuF ₅ NSi	C ₂₀ H ₂₃ AuF ₄ N ₂ Si	C ₄₁ H ₄₆ Au ₂ F ₉ N ₃ Si ₂
Formula Weight	609.46	592.46	1201.92
Crystal Size / mm	0.18×0.070×0.025	0.15×0.077×0.069	0.50×0.050×0.050
Crystal System	orthorhombic	orthorhombic	orthorhombic
<i>a</i> / Å	7.1309(4)	7.20410(10)	7.1510(3)
<i>b</i> / Å	13.7333(8)	13.5498(2)	13.6446(7)
<i>c</i> / Å	21.9704(10)	21.8640(3)	21.9432(9)
<i>α</i> / °	90	90	90
<i>β</i> / °	90	90	90
<i>γ</i> / °	90	90	90
<i>V</i> / Å ³	2151.6(2)	2134.23(5)	2141.05(17)
Space Group	<i>P</i> 2 ₁ 2 ₁ 2 ₁ (#19)	<i>P</i> 2 ₁ 2 ₁ 2 ₁ (#19)	<i>P</i> 2 ₁ 2 ₁ 2 ₁ (#19)
<i>Z</i> value	4	4	2
<i>D</i> _{calc} / g cm ⁻³	1.881	1.844	1.864
Temperature / K	123	150	123
2 θ _{max} / °	58.688	151.766	57.924
μ / cm ⁻¹	69.42 (Mo K α)	138.73 (Cu K α)	69.73 (Mo K α)
No. of Reflections	Total: 13057 Unique: 5096 <i>R</i> _{int} = 0.0360	Total: 11641 Unique: 4287 <i>R</i> _{int} = 0.0539	Total: 9765 Unique: 4546 <i>R</i> _{int} = 0.0310
<i>R</i> ₁ ^a	0.0268	0.0340	0.0247
<i>wR</i> ₂ ^b	0.0581	0.0855	0.0535
GOF ^c	1.008	1.065	1.049
Max./Mini. peak <i>I</i> / Å ³	1.11 e ⁻ /-1.30 e ⁻	0.94 e ⁻ /-1.11 e ⁻	0.79 e ⁻ /-0.93 e ⁻
Flack parameter	0.061(6)	-0.037(10)	-0.011(6)

^a: For data with *I* > 2.00σ(*I*). ^b: For all reflection data. ^c: Goodness of Fit.

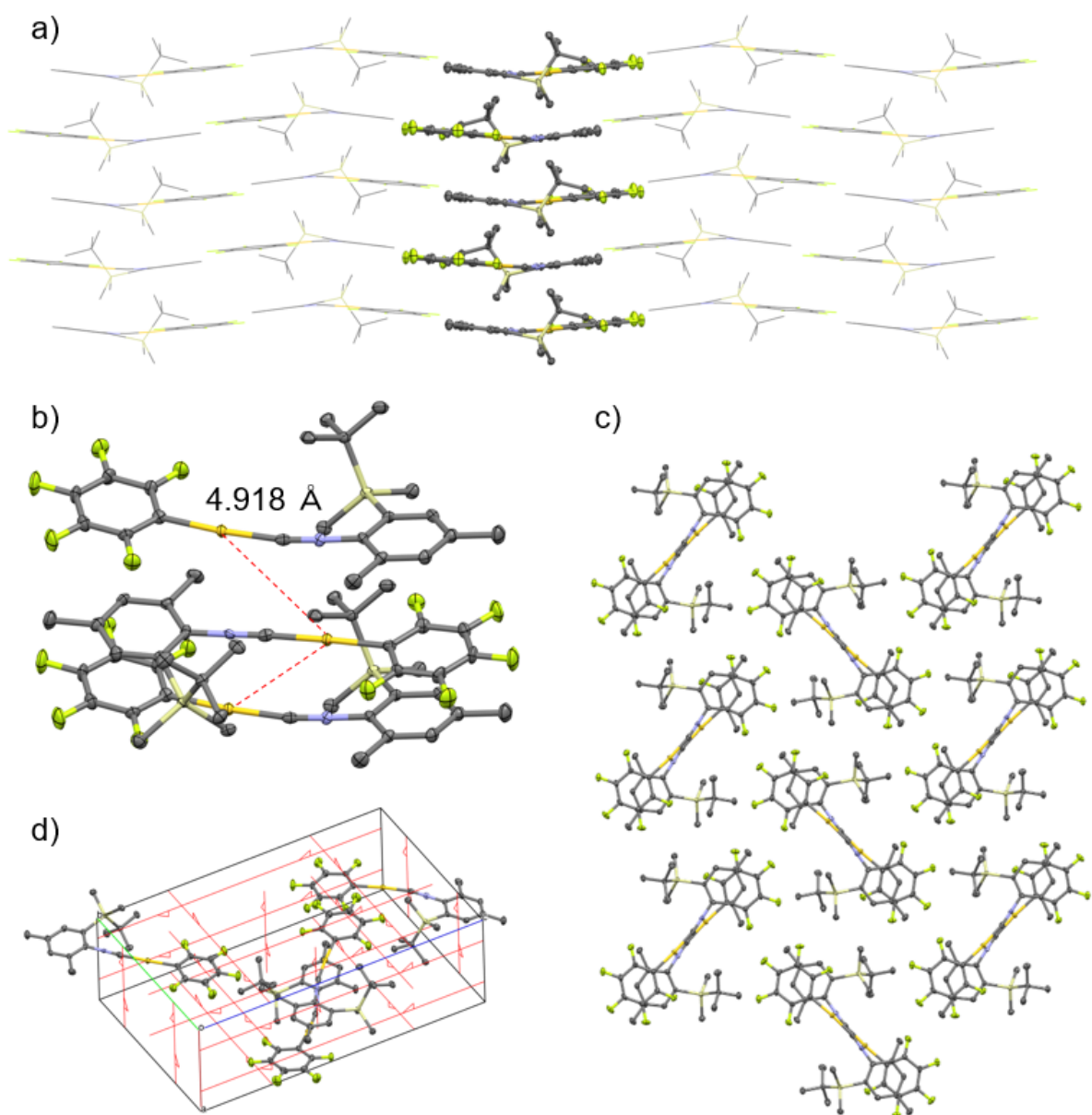


Fig. S7 Single-crystal structure of **1**. H atoms are omitted for clarity.

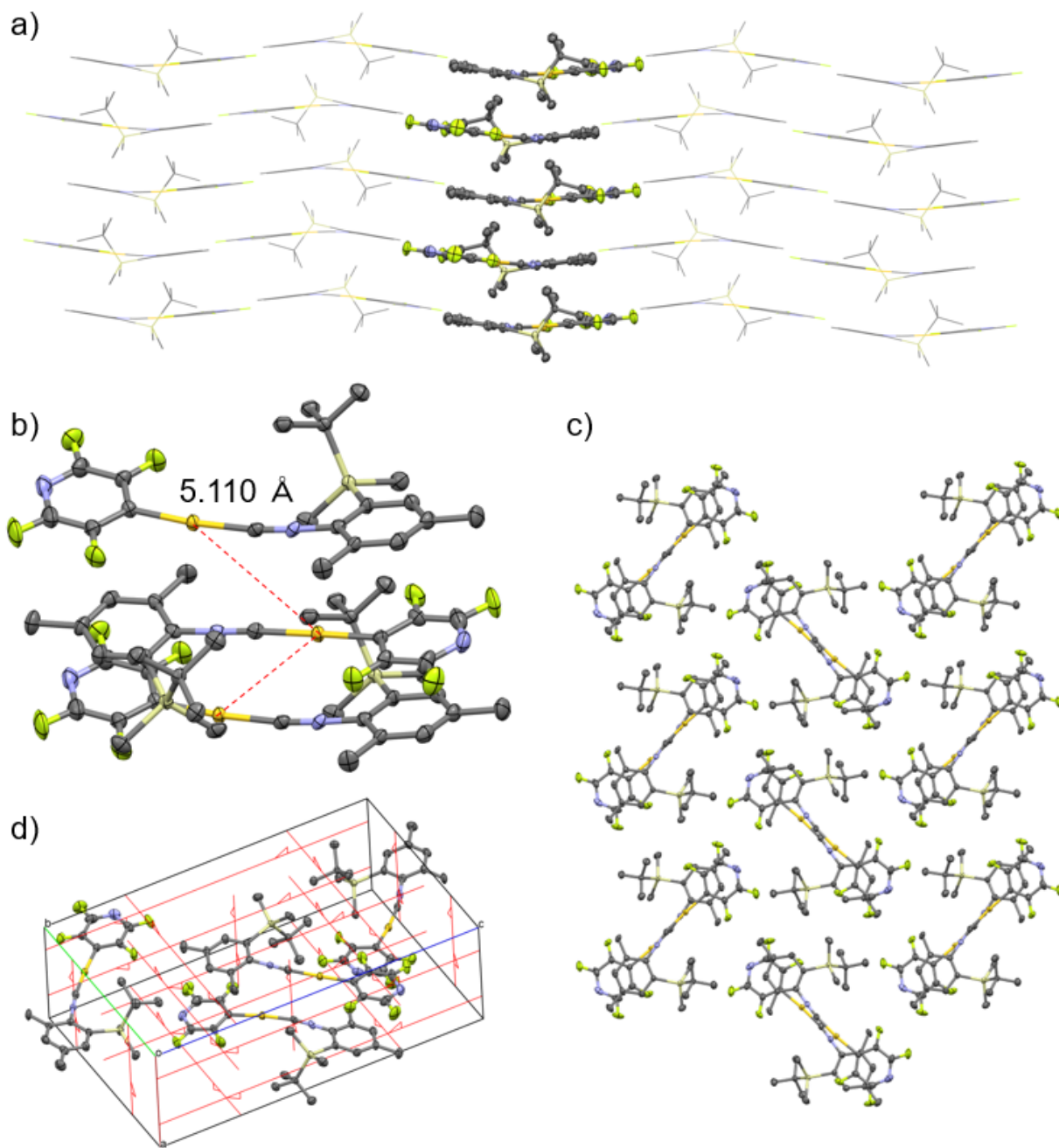


Fig. S8 Single-crystal structure of **2**. H atoms are omitted for clarity.

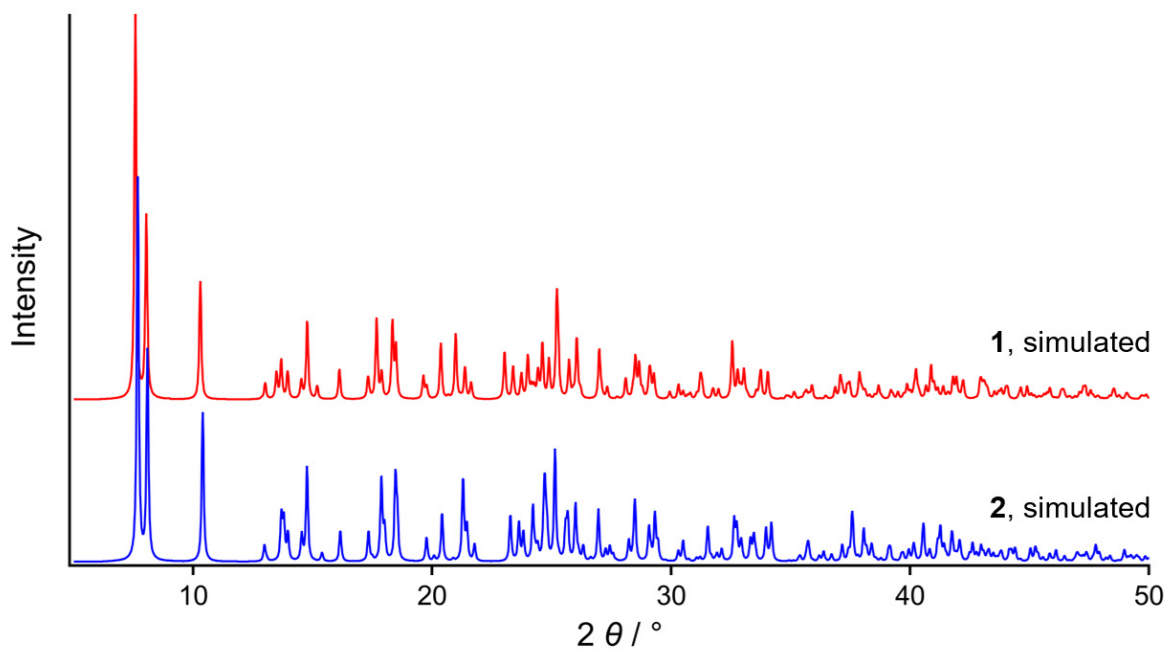


Fig. S9 Simulated powder diffraction patterns of **1** and **2** derived from the single crystal structures.

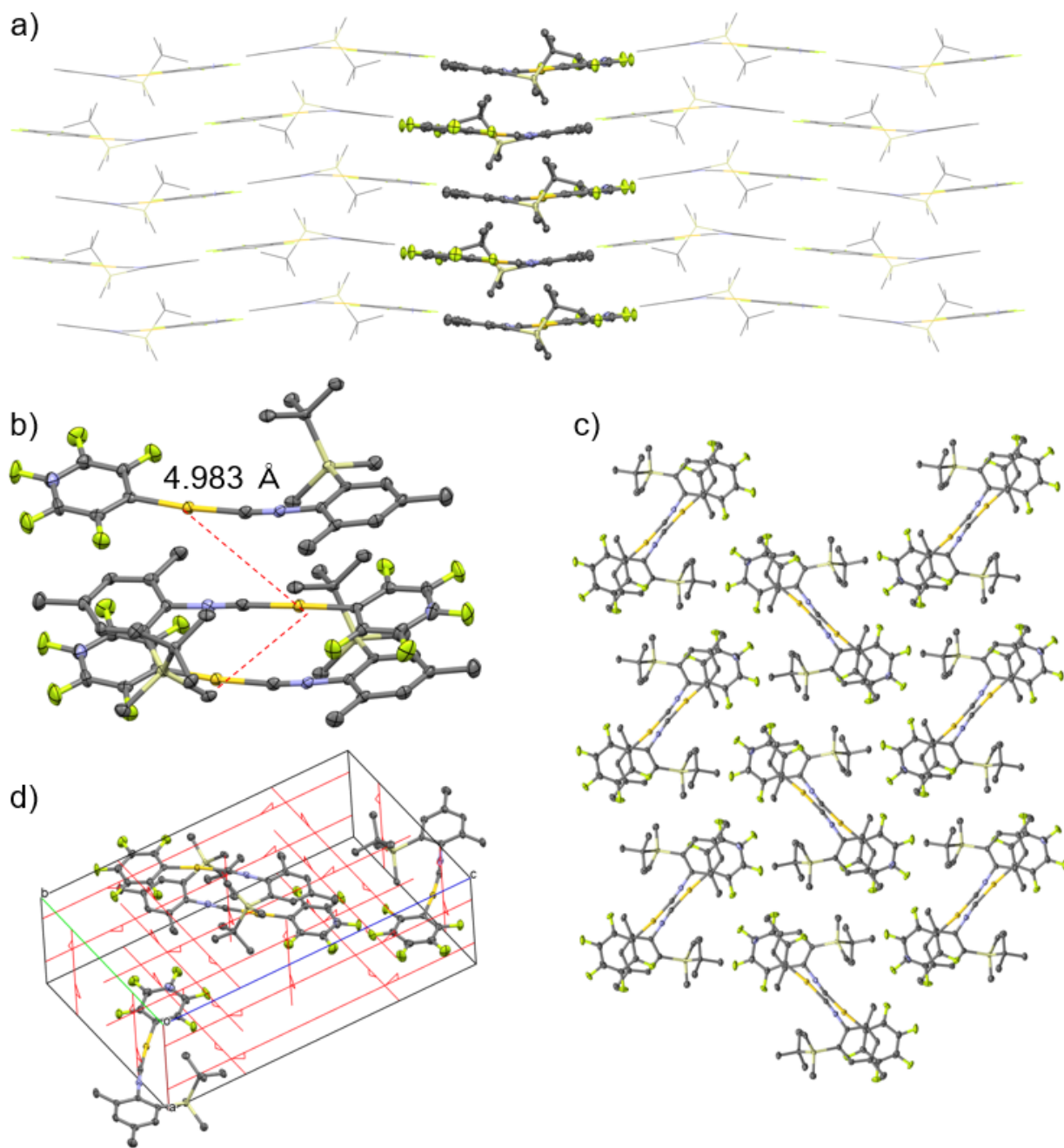


Fig. S10 Single-crystal structure of **1·2**. H atoms are omitted for clarity.

7. ^{19}F NMR spectra of **1**, **2** and **1·2**

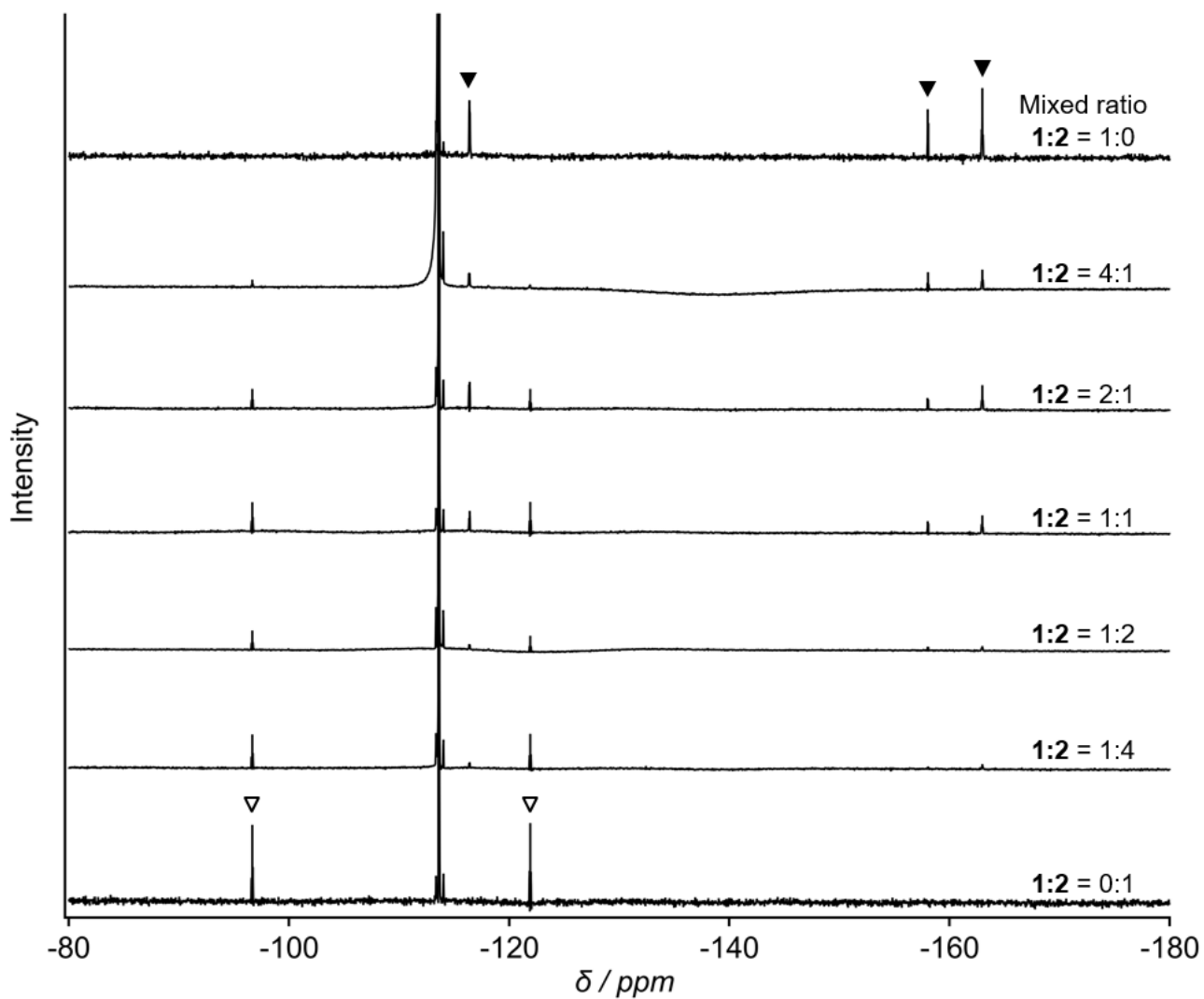


Fig. S11 ^{19}F NMR spectra of **1**, **2** and **1·2** (with a various mixed ratio) in CDCl_3 . The peaks indicated by the filled and opened triangles are attributed to the fluorine signals of **1** and **2**, respectively.

Table S3 Mixed and observed ratios of **1** and **2** in mixed crystals **1·2**

Mixed 1:2 ratio for recrystallization to prepare 1·2	Observed 1:2 ratio in 1·2	
	determined by XRD ^a	determined by ¹⁹ F NMR ^b
4:1	0.80:0.20	0.85:0.15
2:1	0.67:0.33	0.64:0.36
1:1	0.50:0.50	0.50:0.50
1:2	0.33:0.67	0.38:0.62
1:4	0.20:0.80	0.19:0.81

^aThe mixed ratio is determined based on the chemical occupancy values of the disorder moieties in the single-crystal structure analyses. ^bThe mixed ratio is determined based on the integral values of fluorine peaks of **1** (−162.97, −158.02, and −116.38 ppm, see ▼ in Fig. S11) and **2** (−121.91 and −96.67 ppm, see ▽ in Fig. S11) in the ¹⁹F NMR spectra of **1·2**.

8. Emission and Bending Properties of 1·2

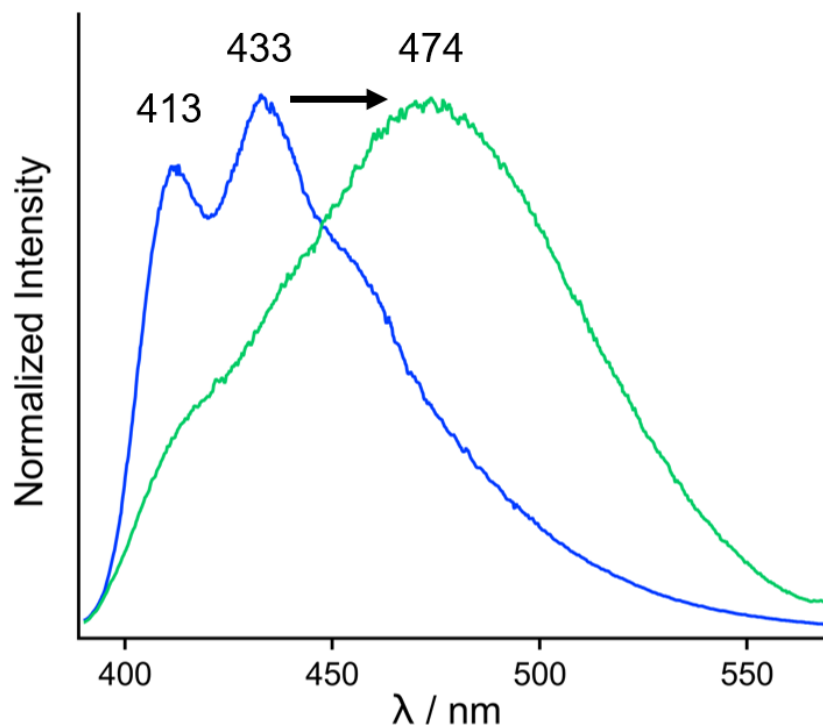


Fig. S12 Emission spectra of solid sample of 1·2 before (blue line) and after (green line) mechanical stimulation.

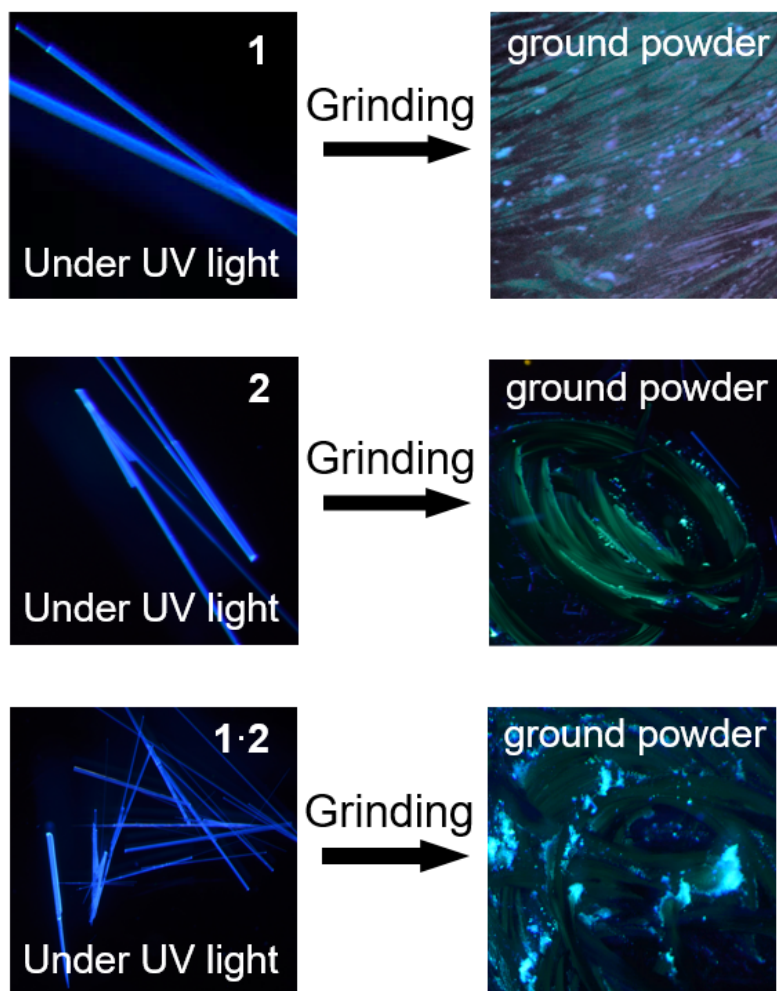


Fig. S13 Photographs of the solid samples of **1**, **2**, and **1·2** before and after grinding. The photographs were taken under UV light (365 nm).

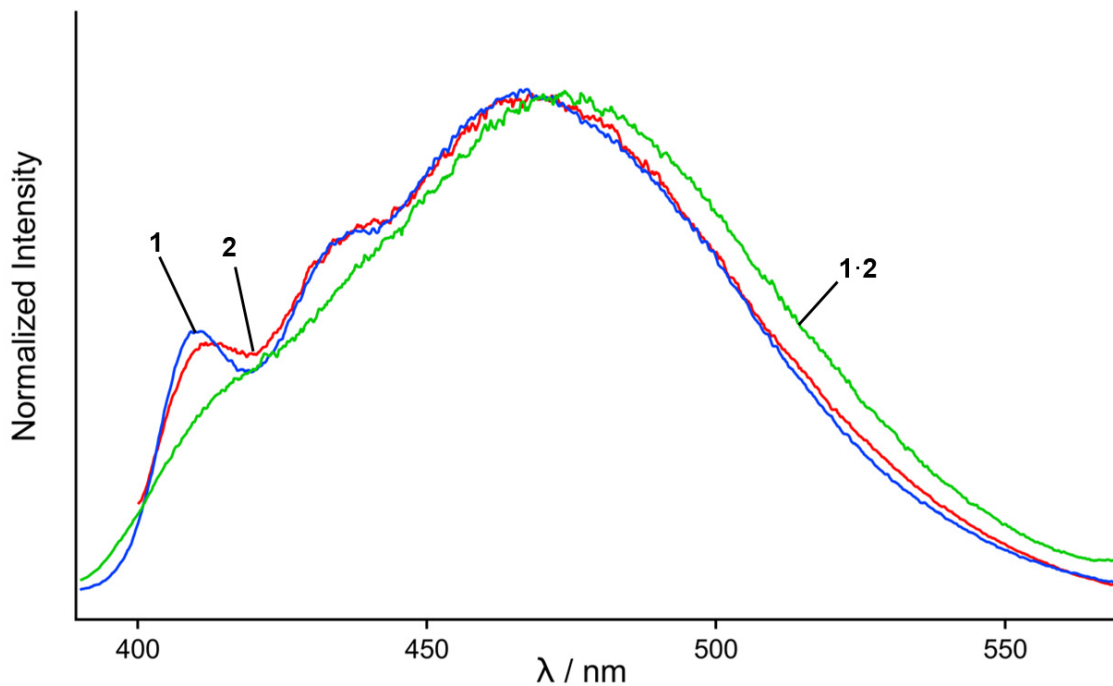


Fig. S14 Emission spectra of solid sample of **1** (blue line), **2** (red line), and **1·2** (green line) after mechanical stimulation.

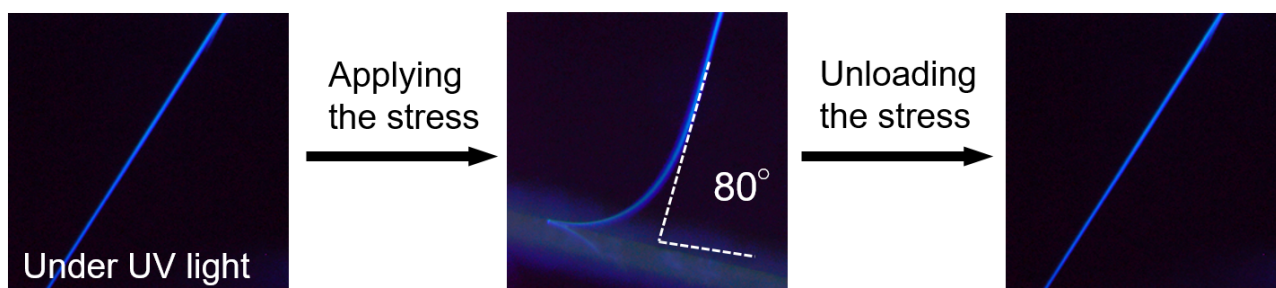


Fig. S15. Photographs of the crystals of **1·2** showing elastic bending property under gentle mechanical stimulation recorded under UV light.

9. NMR Spectra

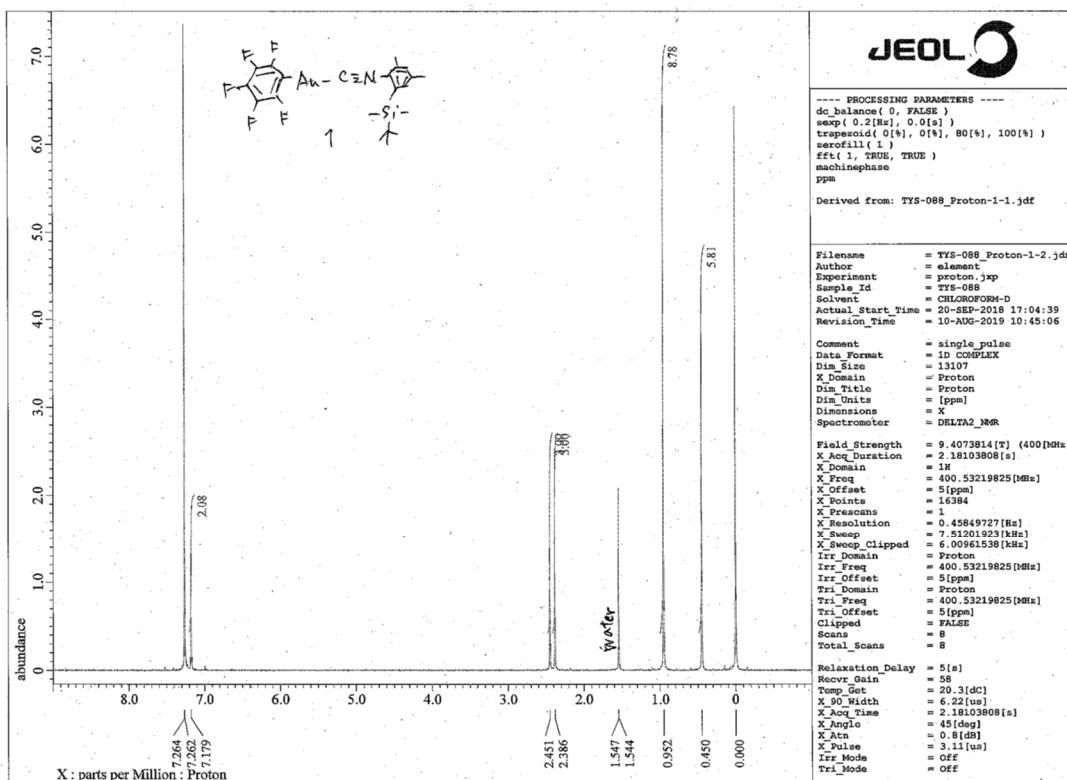


Fig. S16 ¹H NMR spectrum of **1** dissolved in CDCl₃.

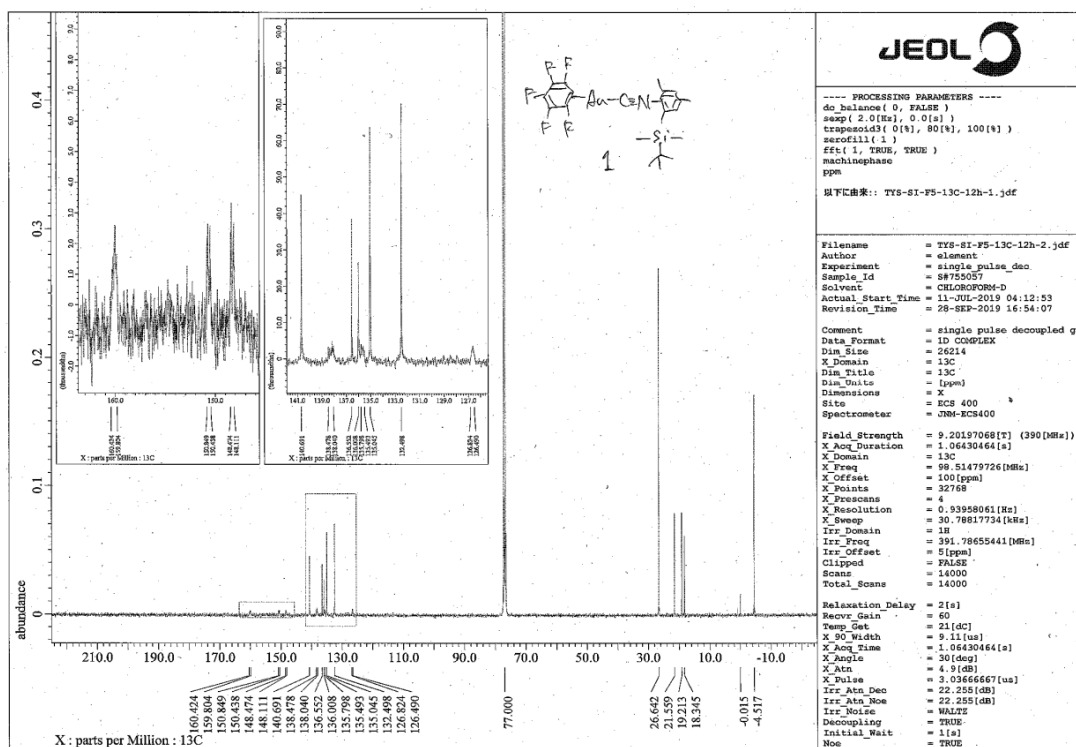


Fig. S17 ¹³C NMR spectrum of **1** dissolved in CDCl₃.

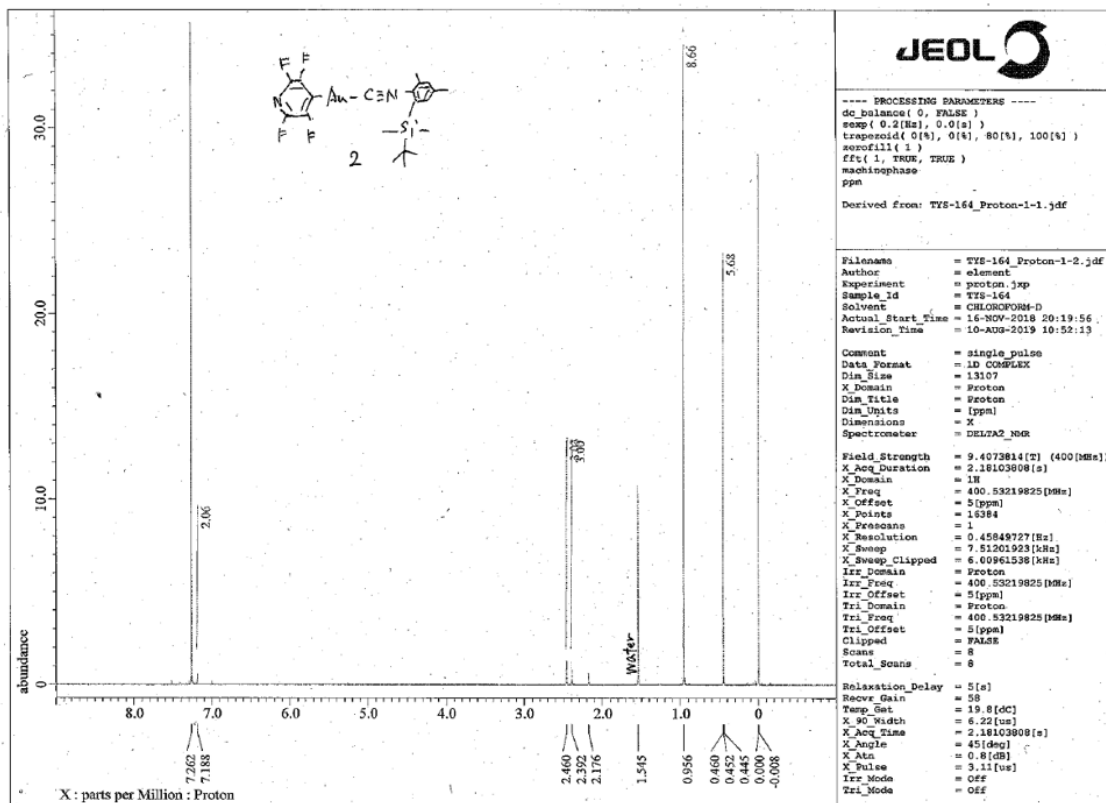


Fig. S18 ¹H NMR spectrum of **2** dissolved in CDCl₃.

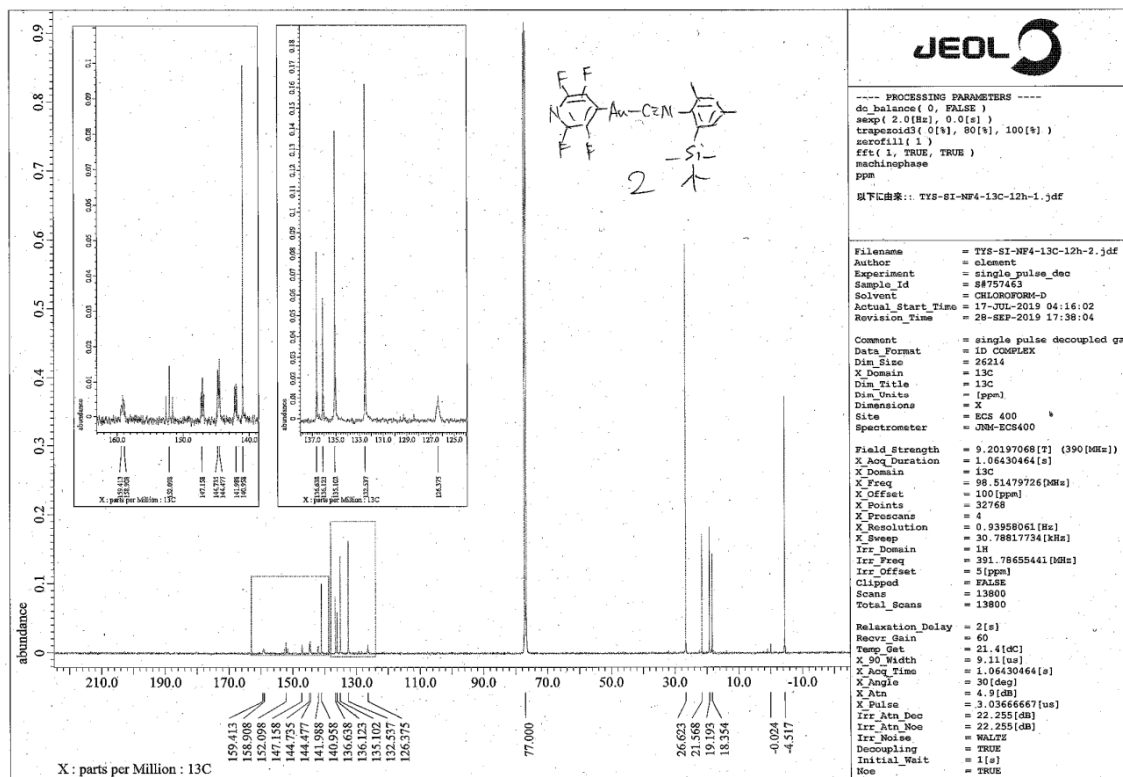


Fig. S19 ¹³C NMR spectrum of **2** dissolved in CDCl₃.

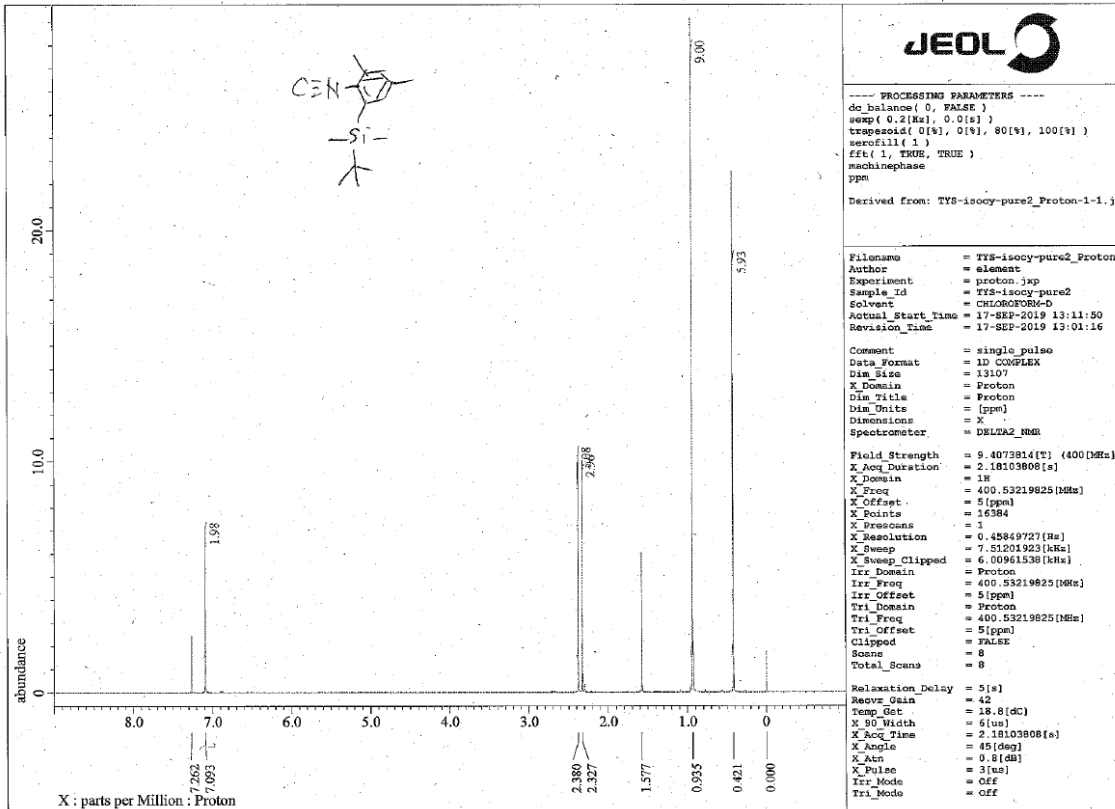


Fig. S20 ¹H NMR spectrum of 3 dissolved in CDCl₃.

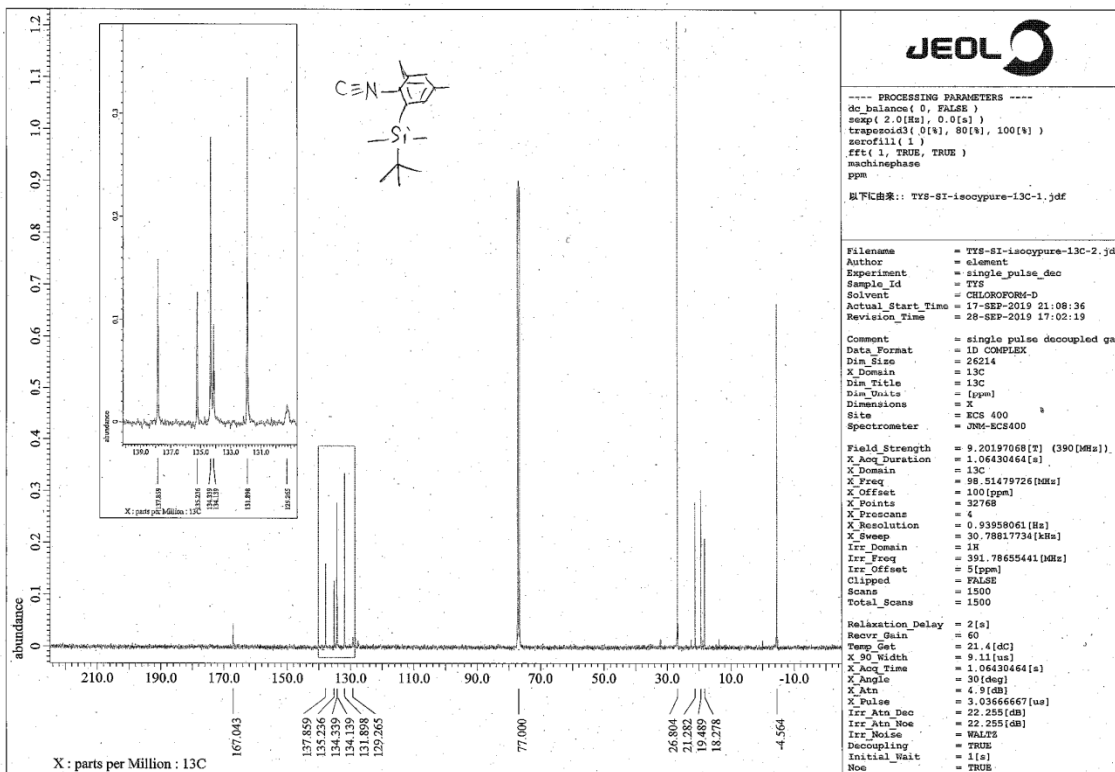


Fig. S21 ¹³C NMR spectrum of 3 dissolved in CDCl₃.

10. References

1. G. M. Sheldrick, *Acta Cryst. Sect. C*, 2015, **71**, 3–8.
2. <https://www.ccdc.cam.ac.uk/support-and-resources/Downloads/>
3. R. Usón, A. Laguna and J. Vicente, *J. Chem. Soc. Chem. Commun.* 1976, 353–354.
4. T. Seki, T. Ozaki, T. Okura, K. Asakura, A. Sakon, H. Uesaka, H. Ito, *Chem. Sci.* 2015, **6**, 2187–2195
5. T. Oe, T. Miyamoto, Y. Ito, T. Ohta, *Chem. Lett.*, 2017, **46**, 1763–1765.